International Journal of Thermophysics, Vol. 9, No. 5, 1988

A Laser Interferometric Dilatometer for Low-Expansion Materials[1]

W. D. Drotning[2]

The development of a high-precision dilatometer based on interferometry presents a number of challenges. This paper describes a laser interferometric dilatometer developed for high-precision thermal expansion measurements in the materials laboratory. The Sandia dilatometer uses dual-beam laser interferometry with a computer-controlled optical alignment feature to achieve high-precision length change measurements. This device has been modified to expand its measurement capabilities in a number of areas. A new thermal chamber has been incorporated which provides a range of measurement from 90 to 500 K while minimizing thermal effects on the optical portion of the instrument. A new specimen holder has been developed to cover this temperature range while accommodating a wider variety of specimen types. In particular, thin (1-mm) composities may be employed in the holder, which uses a single specimen, with only modest shape and preparation requirements, to provide absolute length change measurements. Tilt errors limit the overall performance of dilatometers based on dual-beam interferometry. Significant improvements in precision were demonstrated by incorporating a unique optical system which independently measures specimen holder tilt; tilt errors were corrected and a length change resolution near 0.4 μstrain was achieved. Expansion coefficient data obtained with the device agreed with established results on fused silica and stainless steel. New expansion data were obtained from 90 to 293 K on stainless steel, NBS Standard Reference Material 738.

KEY WORDS: dilatometry; laser interferometric dilatometer; NBS Standard Reference Material 738; stainless steel; thermal expansion.

1. INTRODUCTION

Advanced system designs frequently place stringent dimensional tolerances on structures which undergo severe thermal cycling. Such designs demand low-thermal expansion materials whose thermal properties are known to a

[1] Invited paper presented at the Tenth Symposium on Thermophysical Properties, June 20–23, 1988, Gaithersburg, Maryland, U.S.A.

[2] Sandia National Laboratories, Albuquerque, New Mexico 87185, U.S.A.

0195-928X/88/0900-0849$06.00/0

high precision in order to model the overall structural performance of the system. In space-based structures, for example, the demands for low-weight, high-strength, and low-thermal expansion under wide thermal cycling have led to much interest in the development and measurement of low-expansion composites [1, 2]; frequently, measurements are required in the range of $1 \times 10^{-6}\,K^{-1}$ or lower.

In this paper, we describe a high-precision dilatometer based on laser interferometry, suitable for thermal expansion measurements of low-coefficient of thermal expansion (CTE) materials over the temperature range 90 to 500 K. Several investigators have developed similar dilatometers in recent years, and some discussion of the differences is in order. Tompkins et al. [1] employ an interferometric dilatometer especially suited for measurements on composites, capable of testing a wide variety of specimen geometries in the range 89 to 522 K. For composites, the ability to measure a variety of sizes and shapes is an important device criteria, since specimen preparation must be driven by concern for the ultimate application rather than by measurement requirements. With their choice of interferometer type, Tompkins et al. [1] are able to make measurements at atmospheric pressure, an advantage for some applications. A disadvantage of their instrument is that it is not an absolute device but measures differential expansion of a specimen relative to a known material and, therefore, requires precise expansion information on suitable reference materials. Other interferometric designs incorporate absolute measurements to a high precision [2–5] at the expense of variability of specimen geometry.

The dilatometer described here incorporates (a) the high precision afforded by laser interferometry, (b) absolute length change measurements using a dual-beam interferometer design, (c) a sample holder design which allows a variety of sample sizes and shapes, including thin ($\sim$1-mm) specimens, (d) a wide temperature range of measurement, and (e) automatic control features.

Errors caused by specimen holder tilt can be a significant problem for dilatometers based on interferometric techniques. Fizeau-type interferometers are, by nature, highly insensitive to tilt-induced errors, while dual-beam interferometer methods are not. Optical designs can be used which offer increased tilt immunity [3–6], but the requirements these designs place on the sample size, shape, and preparation can be restrictive. A different approach to reducing tilt errors was employed in this work, where a separate optical system actively detects specimen holder tilt and compensates length change measurements. This unique approach yields improvements to the overall dilatometer performance while retaining the design goal of allowing a wide variety of specimen sizes and shapes with minimal preparation requirements.

2. INSTRUMENT DESIGN

A schematic diagram of the laser interferometric dilatometer is shown in Fig. 1. Major device components are discussed in the following sections.

2.1. Interferometer

The interferometer has been previously described [7, 8]. The dual-beam Michelson interferometer is based around the Hewlett–Packard Model 5526A laser measurement system,[3] which uses an optical heterodyne technique to detect length displacements by ac fringe detection. The instrument resolution is 10 nm. The two interferometer beams are distinguished by their slight difference in frequency and are routed by their respective polarizations. The two interferometer paths (sample and reference) are completed by mirrors which are separated by the length of sample to be measured. Thus, dimensional changes of the specimen in the furnace are mechanically coupled to the interferometer mirrors and are thereby measured by the interferometer.

2.2. Sample Holder

The sample holder is based on the parallel spring arrangement first proposed by Okaji et al. [9] in which the specimen is suported between two blocks which support the two interferometer mirrors. One of the blocks is moveable, responding to specimen length changes, and is supported by two parallel springs which serve to allow mirror motion parallel to the specimen axis. Our design, shown in Fig. 2, embodies significant

[3] Reference to a particular product or company implies neither a recommendation nor an endorsement by Sandia National Laboratories or the U.S. Department of Energy, nor a lack of suitable substitutes.

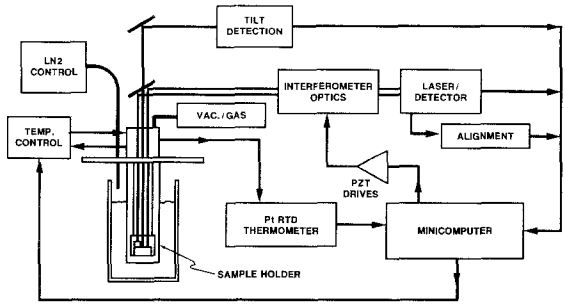

Fig. 1. Schematic diagram of laser interferometric dilatometer.

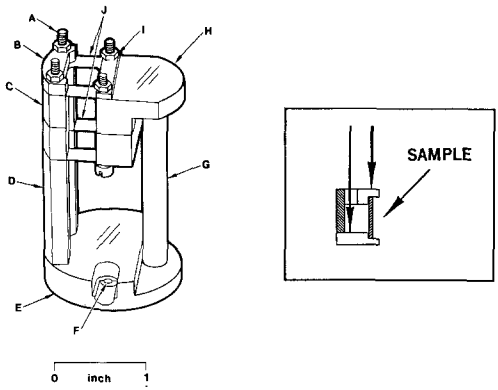

Fig. 2. Parallel spring sample holder/mirror assembly. Inset shows holder cross section, showing relative positions of the sample and the interferometer beams.

changes to the original concept. The structure is rotated to allow use in a vertical configuration. The mirrors E and H are an integral part of the support structure, and the optical path is designed so that the reference interferometer beam passes through the parallel springs J; altogether, a smaller, more compact design results, providing smaller thermal gradients and a symmetric thermal design. In addition, system stability is improved by reducing the number of material interfaces between sample and mirrors. All holder pieces are constructed from low-expansion materials (fused silica and Invar), allowing a wider temperature range of measurement with minimal thermal stress. The inset in Fig. 2 displays the side view of the holder, showing the relative positions of the sample and interferometer beams. Upper and lower sample supports (E and H) are ground from multilayer dielectric coated fused silica laser mirrors (CVI Inc., Albuquerque, N.M.). The parallel springs J were constructed from a 0.05-mm Invar sheet. Invar support stack D may vary in height to accommodate different sample lengths; a 51-mm specimen is shown. The specimen may rest against the steps in the mirror supports should it be unable to stand alone. The effective force on the sample is typically 10 g. Vertical excursions of the upper mirror in excess of 0.5 mm have been demonstrated while maintaining sufficiently parallel motion to maintain fringes detectable by the interferometer system.

2.3. Optical Detection of Tilt

The inset in Fig. 3 illustrates the two interferometer beams reflecting from a single mirror. Of the possible rotations and translations of the

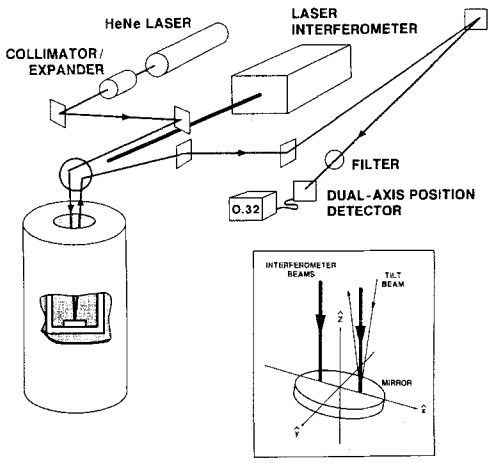

Fig. 3. Optical schematic of tilt detection system. Inset shows detail of interferometer and tilt beams.

mirror, only rotational tilt around the y axis is detectable by the interferometer, and it is indistinguishable from relative displacement of the interferometer beams along the z axis. Therefore, any y-axis rotation of the entire system can contribute to error in the displacement to be measured.

The present device corrects for such tilt errors by a unique method of active detection and compensation. As shown in Fig. 3, a separate HeNe laser beam is collimated, expanded, and directed onto the lower interferometer mirror. The tilt beam is not collinear with the reference beam but forms a slight angle in the yz plane. On reflection, the tilt beam is detected some 4 m away by a dual-axis position sensitive detector (UDT Model SC-25D, United Detector Technology, Hawthorne, Calif.) and amplifier (UDT Model 301-DIV). With this scheme, mirror rotation about y translates to horizontal motion at the detector; the detection resolution corresponds approximately to a 2-μrad tilt. By direct calibration, a position detector voltage shift thus corresponds to vertical displacement error.

Mirror rotation about the x axis and displacement along z cause vertical motion of the tilt beam at the position detector but no horizontal motion. Thus, the error-producing tilt is decoupled from other sources of tilt beam motion, such as thermal expansion of the entire assembly which causes displacement of the mirror along z, common to both sample and reference interferometer beams. Thermal uniformity of the tilt detection optical system is important to eliminate extraneous beam motion at the detector.

2.4. Thermal System

The thermal control and measurement system is depicted in Fig. 1. Detail of the specimen heater is shown in Fig. 4. The heater comprises a solid copper block N with a stainless steel-sheathed wire heater S (300 W, ARi Industries Aerorod heater, BXD-09F-88) vacuum brazed to the copper block. Heater temperature is regulated by a proportional controller using a Type K thermocouple R. The sample holder O is situated inside the covered heater block, which is held in the vacuum chamber K. Low-pressure (1-Torr) helium is used to provide thermal equilibration. The vacuum chamber is surrounded by liquid nitrogen. Vertical temperature gradients along a sample were measured at less than $0.2\ \mathrm{K \cdot cm^{-1}}$ in most cases.

Specimen temperatures are determined from a calibrated platinum resistance thermometer Q (RTD). The RTD (Model 1PT100G1230,

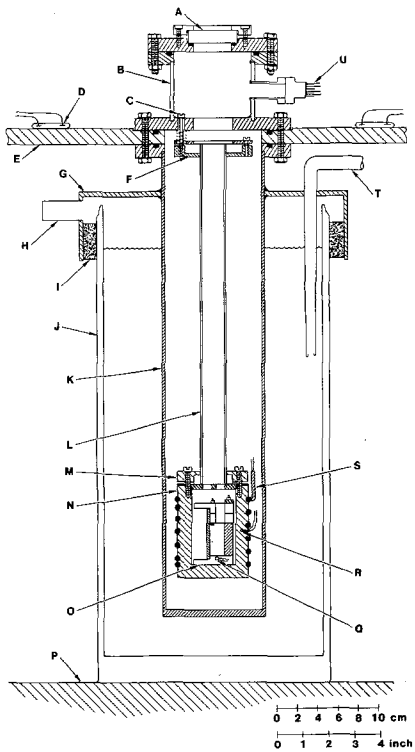

Fig. 4. Vertical cross section of mechanical assembly of specimen chamber, support structure, and thermal system.

Omega Engineering, Inc., Stamford, Conn.) is wound inside glass and is placed inside the lower mirror of the sample holder (F; Fig. 2). The RTD conforms to standard DIN 43760 and is measured with a four-wire resistance technique by a digital thermometer (Fluke Model 2180A). Following calibration, specimen temperature uncertainty is 0.4 K; measurement precision is estimated at 0.2 K.

2.5. Mechanical System

The sample holder and heater block are held inside the vacuum chamber K by a fused quartz tube L which is clamped at both ends (M and F) and attached to the upper vacuum chamber B by means of the adjustable tripod support C. Optical access is through the quartz window A. The entire chamber is evacuated and backfilled with helium and is supported by a plate E which is attached to a vibration-isolated optical table. Heaters D are controlled at 311 K to assist in thermal stabilization of the support structure. The optical table is contained in a thermal enclosure, maintained at 298 ± 0.2 K by circulating air. The entire dilatometer system is in a temperature-controlled room.

The liquid nitrogen dewar J is supported by plate P, also attached to the optical table. The dewar is covered with a cap G and seal I. Cold nitrogen gas is vented from the thermal enclosure at port H to minimize thermal fluctuations. The space between plate E and cap G is insulated as well. Liquid nitrogen is introduced through port T under a low fill pressure. This is accomplished through an automatic dual-control fill system, in which a supply dewar fills an intermediate nitrogen dewar, which then fills the experiment dewar J by gravity feed. This dual-control system has the effect of eliminating disturbances to the dilatometer system during cryostat filling, caused by vibration and pressurized venting of cold gas.

2.6. Computer Controller

The dilatometer system is controlled by a Hewlett–Packard 1000 A-Series minicomputer. Interfacing is accomplished through IEEE-488 interface buses or by onboard D/A and A/D converters in the computer, depicted in Fig. 1. The RTE-A operating system is used for real-time multitasking control of the instrument. System programs were developed which allow the computer simultaneously to acquire length and temperature data, perform on-line tilt compensation, monitor and control optical alignment of the interferometer, and perform complete temperature cycling control. The computer also handles all data analysis and presentation functions.

3. PERFORMANCE

Dilatometer performance is discussed in this section in terms of the individual contributions from interferometer resolution and stability, temperature precision, and the tilt compensation system. Overall performance is also discussed in the next section, where measurements on thermal expansion standards are presented.

A number of investigators have performed detailed precision analysis of interferometric dilatometers of similar design [2–6, 10]. Error due to laser stability and fringe fraction determination are typically much smaller than the 10-nm resolution of the current instrument. Our length change uncertainty is dominated by long-term system stability for an isothermal system [11] and by the tilt compensation performance during thermal cycling of the apparatus. Under isothermal conditions, interferometer path length was found to be stable to within ± 20 nm over 24 h, based on measurements from a single mirror in the sample chamber.

The current sample support design results from testing and modification of several approaches and reflects the best performance for measured length changes during thermal cycling of a single mirror (a so-called "zero drift" or "baseline" test). Even with the present design, baseline shifts of as much as 1 μm were still observed over 300 K temperature spans; in addition to the magnitude of these shifts, they were not sufficiently reproducible to allow a temperature-dependent baseline correction. The source of the baseline shifts was determined to be due to mirror rotation about a horizontal axis. As a result, the tilt compensation system described above was devised. An example of the tilt correction performance is shown in Fig. 5, where raw and tilt-compensated length results are compared.

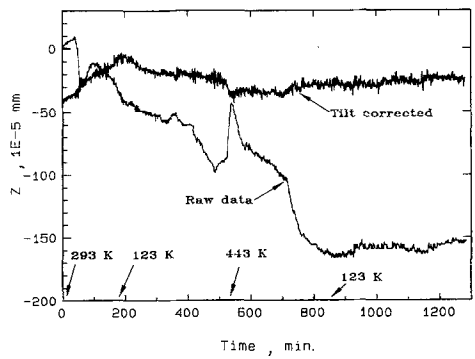

Fig. 5. Baseline (measured displacement using a single mirror) vs time, showing effect of tilt correction to raw data. Temperature profile is indicated along abscissa.

Figure 5 demonstrates the range of correction afforded by the tilt compensation system. The test depicted was particularly severe; during the initial 200 min, the dewar was filled, causing start-up thermal disturbances. The sharp spike at 550 min reflects a rapid shutdown of the furnace due to an over-temperature condition. During other regions of the test, heating and cooling rates of $1\ \mathrm{K \cdot min^{-1}}$ were accomplished, resulting in rms length variations of ± 30 nm, after tilt compensation, over substantial temperature ranges. Over smaller temperature ranges (typically a 40 K span is used for CTE measurements between isotherms), baseline variations of 10–20 nm have been observed, near the resolution of the interferometer. For 50-mm specimens, the figure of 20 nm translates to a detection limit of 0.4 μstrain.

For most materials, temperature measurement uncertainty is the dominant contributor to CTE uncertainty [4–6]. After thermometer calibration and correction for thermometer-to-specimen gradients, an imprecision of ± 0.2 K remains. For a material with a CTE of $1 \times 10^{-5}\ \mathrm{K^{-1}}$ and a length of 50 mm, measured over a temperature span of 40 K, the overall estimated uncertainty in CTE is $\pm 0.72\%$, or $\pm 7.2 \times 10^{-8}\ \mathrm{K^{-1}}$. Similarly, for a CTE of $1 \times 10^{-6}\ \mathrm{K^{-1}}$, the uncertainty is $\pm 1.6\%$, or $\pm 1.6 \times 10^{-8}\ \mathrm{K^{-1}}$.

4. RESULTS AND DISCUSSION

Several low-CTE and standard materials were investigated to evaluate the overall dilatometer performance; results for two materials are presented here. CTE data were obtained by direct measurement between isotherms, typically 40 K apart. The computer monitored temperature and corrected length data for stability during isothermal equilibration, which typically was achieved in 30 to 200 min. A stable isotherm was determined when time-averaged data yielded standard deviations less than preset values, chosen to achieve a CTE uncertainty less than $3 \times 10^{-8}\ \mathrm{K^{-1}}$. A finite temperature interval correction was applied to each CTE value, following the method of Hahn [12]. CTE values were determined on heating and cooling, in random order throughout the investigated temperature range, with multiple specimen insertions.

4.1. Fused Silica—NBS SRM 739

Two 50.8-mm fused silica NBS [13] Standard Reference Materials (SRM) were measured in the dilatometer. Near 173 K (-100°C), the CTE of fused silica (SRM 739) changes sign, thereby presenting an excellent material for low-CTE investigation of the device. Figure 6 shows the CTE data of several measurements on one specimen, with and without the tilt

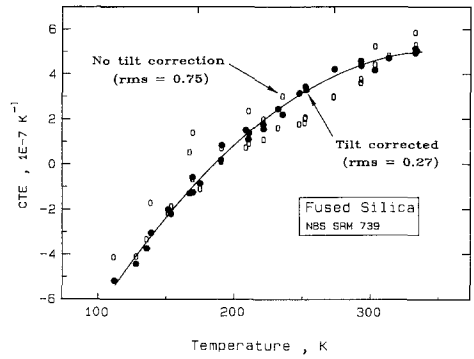

Fig. 6. CTE of fused silica SRM 739, with (filled circles) and without (open circles) tilt correction.

correction applied to the length data. The significant scatter in the data was reduced threefold by use of the tilt compensation method, as determined from the rms fit deviations.

Figure 7 shows all CTE data obtained on SRM 739 in this study. No specimen variations were observed. Data below 373 K (100°C) were least-squares fit to a cubic polynomial, given by

$$\text{CTE} = -15.952 + 0.1148\,T - 1.516 \times 10^{-4}\,T^2 - 8.2008 \times 10^{-9}\,T^3$$

where CTE is in $10^{-7}\,\text{K}^{-1}$ and T is in K. The rms deviation of the fit was $2.7 \times 10^{-8}\,\text{K}^{-1}$ from 91 data points, near the estimated device uncertainty. Also displayed is the segmented cubic fit from NBS for the standard. Our data are systematically lower than the NBS fit, typically by $4 \times 10^{-8}\,\text{K}^{-1}$, although the difference is within the combined error of both sets of

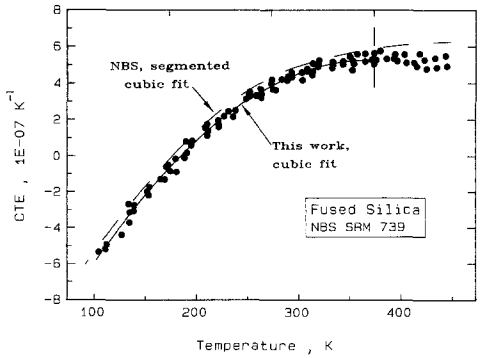

Fig. 7. CTE vs temperature for fused silica SRM 739, with cubic least-squares fit (solid line) below 373 K. Dashed line is NBS segmented cubic fit.

measurements and is smaller than observed by other investigators [14]. Data above 373 K for these particular specimens are shown for information but were judged to be invalid because the specimen length was not sufficient to match the rapidly increasing expansion of the Invar which supports the specimen mirror. Above 440 K, the mirror lost contact with the specimen. Depending on the expected expansion of the sample and the temperature range, the specimen length must be carefully considered, relative to the Invar stack height, in order to eliminate this concern.

4.2. Stainless Steel—NBS SRM 738

Measurements were obtained from 93 to 433 K on the recently certified NBS SRM 738, an AISI 446 stainless-steel standard, 50.8×6.4 mm. The least-squares fit to our data, shown in Fig. 8, is given by:

$$\text{CTE} = -7.2349 + 0.1819\,T - 8.0558 \times 10^{-4}\,T^2 + 1.6943 \times 10^{-6}\,T^3 - 1.3561 \times 10^{-9}\,T^4$$

where CTE is in $10^{-6}\,\text{K}^{-1}$; the rms deviation is 0.041. Differences from the NBS results range from $2 \times 10^{-7}\,\text{K}^{-1}$ at 293 K to 0 at 373 K. Unlike the NBS values, which show a linear CTE dependence on temperature, our data show a significant curvature near 293 K, which becomes more evident at subambient temperatures. The overall trend with temperature is similar to the TPRC curve, which represents the recommended curve given by the Thermophysical Properties Research Center [15] for similar classes of steel alloys. The present results on SRM 738 below 293 K indicate that the material may serve as a suitable low-CTE reference for applications which require metals.

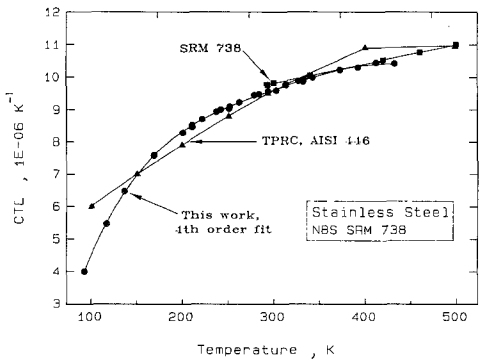

Fig. 8. CTE vs temperature for stainless steel, NBS SRM 738 (circles), with fourth-order fit. SRM values (squares) and typical AISI 446 alloy steel results [15] (triangles) are also displayed.

5. SUMMARY

A laser interferometric dilatometer was developed to operate over the range 90 to 500 K (−180 to 230°C). A parallel spring sample holder/mirror assembly was designed to allow absolute displacement measurements on samples of widely varying geometry, including thin (1-mm) specimens. Significant performance improvements were obtained by employing a unique tilt compensation system, in which an active optical system detects and corrects tilt-induced displacement errors. Length change resolution of 0.4 μstrain was achieved. Expansion coefficient data obtained with the device agreed with established standards. New expansion data were obtained from 90 to 293 K on stainless steel, NBS Standard Reference Material 738.

ACKNOWLEDGMENTS

We are grateful to T. V. Tormey for his contributions to the design and construction of the dilatometer. This work, performed at Sandia National Laboratories, was supported by the U.S. Department of Energy under Contract DE-AC04-76-DP00789.

REFERENCES

1. S. S. Tompkins, D. E. Bowles, and W. R. Kennedy, *Exp. Mech.* **26**:1 (1986).
2. E. G. Wolff and R. C. Savedra, *Rev. Sci. Instrum.* **56**:1313 (1985).
3. S. J. Bennett, *J. Phys. E Sci. Instrum.* **10**:525 (1977).
4. K. P. Birch, *J. Phys. E Sci. Instrum.* **20**:1387 (1987).
5. M. Okaji and H. Imai, *J. Phys. E Sci. Instrum.* **20**:887 (1987).
6. M. Okaji and H. Imai, *J. Phys. E Sci. Instrum.* **17**:669 (1984).
7. W. D. Drotning, in *Thermal Expansion 7*, Proceedings of the Seventh International Thermal Expansion Symposium, D. C. Larsen, ed. (Plenum Press, New York, 1982).
8. W. D. Drotning, Report SAND83-0197 (Sandia National Laboratories, Albuquerque, N.M., May 1983). (Available from National Technical Information Service, U.S. Department of Commerce, 5285 Port Royal Road, Springfield, Va. 22161.)
9. M. Okaji, H. Imai, N. Hida, and K. Iizuka, in *Thermal Expansion 8*, Proceedings of the Eighth International Thermal Expansion Symposium, T. A. Hahn, ed. (Plenum Press, New York, 1984).
10. H. Imai and W. J. Bates, *J. Phys. E Sci. Instrum.* **14**:883 (1981).
11. W. D. Drotning, *Rev. Sci. Instrum.* **52**:1896 (1981).
12. T. A. Hahn, *J. Appl. Phys.* **41**:5096 (1970).
13. National Bureau of Standards Certificate, Office of Standard Reference Materials, Gaithersburg, Md.
14. T. A. Hahn and R. K. Kirby, in *Thermal Expansion—1971*, Proceedings of the 1971 Thermal Expansion Symposium, AIP Conf. Proc. No. 3, M. G. Graham and H. E. Hagy, eds. (Am. Inst. Phys., New York, 1972).
15. Y. S. Touloukian, R. K. Kirby, R. E. Taylor, and P. D. Desai, *Thermophysical Properties of Matter, Vol. 12* (Plenum Press, New York, 1975).